European Review for Medical and Pharmacological Sciences 2019; 23: 5874-5883

Combined mTOR/MEK inhibition prevents proliferation and induces apoptosis in NF2-mutant tumors

N. LI[1], X.-Y. LU[2], W.-Y. SHI[1], F.-J. MAO[1], X.-Y. YANG[1], Y.-B. LUO[2], W. LI[1]

[1]Department of Scientific Research, Shanghai Municipal Hospital of Traditional Chinese Medicine, Shanghai University of Traditional Chinese Medicine, Shanghai, China
[2]Department of Oncology, Shanghai Municipal Hospital of Traditional Chinese Medicine, Shanghai University of Traditional Chinese Medicine, Shanghai, China

Ning Li, Xinyi Lu and Fajiang Mao equally contributed to this work

Abstract. – OBJECTIVE: Merlin is encoded by Neurofibromatosis type 2 gene (NF-2), a tumor suppressor gene, which causes some multiple tumors forming disease of the nervous system in case of function loss. Bioinformatics analysis suggested that patients with NF-2 mutation had a worse prognosis, while it was associated with PI3K/mTOR activation, implying abnormal apoptosis in NF-2 mutation related tumors. Hence, we supposed that the inhibitors of PI3K/mTOR pathway might play a role in suppressing the tumor proliferation.

MATERIALS AND METHODS: Two representative NF-2 mutation tumor model of NCI-H2452 and HEI193 cell lines were adopted, while two PI3K/mTOR pathway inhibitors Trametinib and Vistusertib were chosen to study the proliferation and apoptosis of the tumor cells.

RESULTS: CCK8 cell counting experiment showed that both Trametinib and Vistusertib could inhibit the proliferation of NCI-H2452 cell *in vitro*, while the combination of Trametinib and Vistusertib was more significant. Flow cytometry results showed that both Trametinib and Vistusertib could enhance apoptosis of NCI-H2452 cell *in vitro*, while the combination of Trametinib and Vistusertib was more significant. Similar results were also achieved for HEI193 cell lines. *In vivo* tumorigenicity experiments demonstrated that the tumor volume and weight were significantly decreased by both Trametinib and Vistusertib, while their combination had the most significant effect. Western blot results demonstrated that both Trametinib and Vistusertib could inhibit PI3K/mTOR /MEK pathway and enhance the expression of merlin.

CONCLUSIONS: We found that PI3K/mTOR inhibitor could decrease the proliferation of NF-2 mutation tumor cell lines by enhancing apoptosis, while the combination of two drugs might have a better effect.

Key Words:
Neurofibromatosis type 2 gene, PI3K/mTOR pathway, Trametinib, Vistusertib, Proliferation, Apoptosis.

Introduction

Gene mutation plays a key role in the development, metastasis and recurrence of tumors, which can be divided into oncogene and tumor suppressor gene according to their functions[1]. NF-2 gene is one of the most common and studied tumor suppressor genes, which encodes a membrane-cytoskeleton scaffolding protein – merlin[2]. Mutation in NF-2 gene or function loss of merlin can cause Neurofibromatosis type 2 (NF2), a nervous system tumor-forming disease[3]. However, NF-2 gene mutation is also very common in other types of malignant tumors, including renal cell carcinoma[4,5], malignant pleural mesothelioma[6], sporadic spinal schwannoma[7], urothelial carcinoma[8], liver tumor[9], ependymal tumors[10], colorectal cancer [11]. Hence, targeting NF-2 mutation might provide some therapeutic sites or clues for cancer treatment. Online tumor database analysis showed that NF-2 mutation was associated with PI3K/mTOR pathway activation, which implied that NF-2 mutation related tumors might derive from inhibition of apoptosis[12]. Trametinib is a selective mitogen-activated extracellular signal-regulated kinase (MEK) inhibitor, which was used for the treatment of BRAF V600-positive melanoma[13]. Vistusertib is a dual m-TORC1/2 inhibitor, which was used for the treatment of high-grade serous ovarian cancer (HGSOC) and squamous non-small-cell lung cancer (sqNSCLC)[14]. HEI193 cells and

Corresponding Author: Wei Li, MD; e-mail: blacklining@136.com

NCI-H2452 cells are the most commonly used cell lines for the study of NF-2 mutation[15,16]. However, there was no previous study focusing on the effect of PI3K/mTOR inhibitor on NF-2 mutation related tumors. In this study, we investigated the effect of PI3K/mTOR pathway inhibitor on the proliferation of NF-2 mutation related tumors, as well as its potential mechanisms.

Materials and Methods

Bioinformatics Analysis

To figure out the expression of NF-2, a total of 118 neurofibromatosis tissue samples that contained the expression of NF-2 were collected from TCGA database (http://cancergenome.nih.gov/)[17]. Long-term prognosis information was also collected to analyze the association with NF-2 expression level. Finally, the expression of NF-2 of neurofibromatosis tissues and the long-term prognosis was analyzed using GraphPad Prism 5.01 software (GraphPad Software Inc., La Jolla, CA, USA). The results demonstrated that patients with lower NF-2 level had a significantly worse prognosis than those with higher NF-2 level (p=0.03) (Figure 1A). The Search Tool for the Retrieval of Interacting Genes/Proteins (STRING) database (http://string-db.org/) consolidates known and predicted protein-protein association data for a large number of organisms, contributing to uncovering the direct (physical) and indirect (functional) relationships of NF-2. In the present study, PPI network of common DEGs was constructed by the latest STRING v10.5 database based on a minimum required interaction score 0.7. PPI network with the most number of nodes was visualized by Cytoscape v3.3.0 software[18] (Figure 1B). STRING results demonstrated that NF-2 was significantly associated with PI3K/mTOR/MEK pathway.

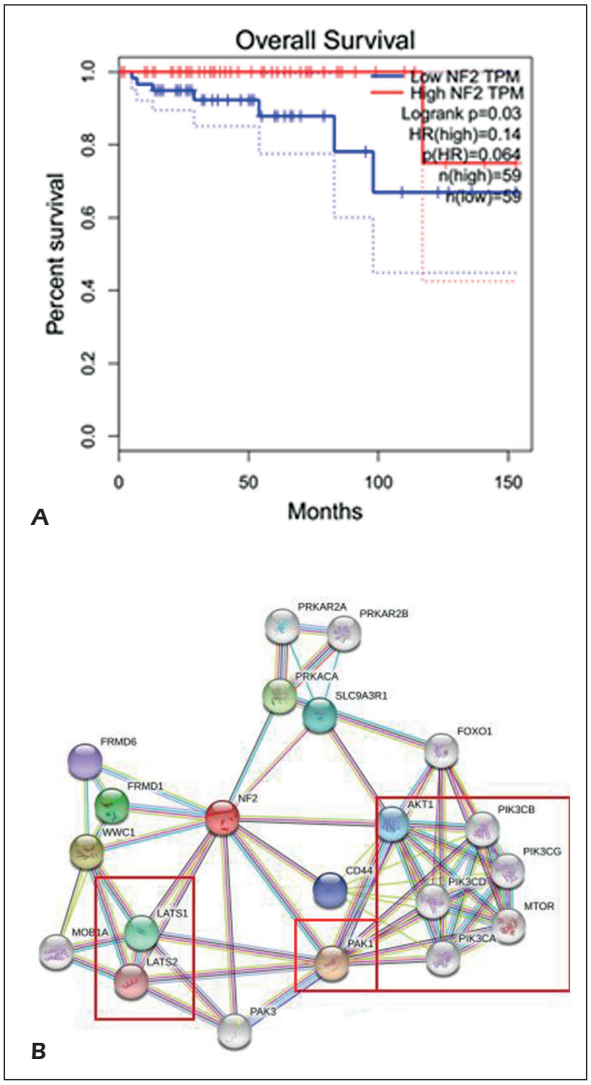

Figure 1. Bioinformatics analysis of NF-2 mutation. **A**, Survival analysis of patients with low or high NF-2 level from TCGA database. **B**, NF-2 mutation was linked to PI3K/mTOR pathway from STRING database.

Cell Proliferation Inhibition

Cell Culture

HEI193 cell lines and NCI-H2452 cell lines were purchased from Shanghai Guandao Biological Engineering Co., Ltd. (Shanghai, China). HEI193 cells were maintained in Dulbecco's Modified Eagle's Medium (DMEM), which contained 10% fetal bovine serum (FBS) and 100 U/ml penicillin and 100 microg/mL streptomycin. NCI-H2452 cells were maintained in Roswell Park Memorial Institute-1640 (RPMI-1640) medium supplemented with 10% fetal bovine serum (FBS). To maintain cell morphology, the cells were used at passage six, while a hemocytometer was used to calculate cell number. All cells were cultured at 37°C with 5% CO_2 and 100% humidity. All the above products were purchased from Gibco (Life Technologies/Gibco, Carlsbad, CA, USA).

IC50 Detection

HEI193 cells and NCI-H2452 cells were seeded in 96-well plates and treated with varying concentrations of Trametinib (Mekinist, purchased from GlaxoSmithKline Inc., Rockville,

MD, USA) and Vistusertib (AZD2014, purchased from the Pharmaceutical Company, USA) for 72 hrs. Both compounds were dissolved in dimethyl sulfoxide (DMSO) and stocks of 1 mM diluted in DMEM1X were used for *in vitro* experiments. Compound concentrations were tested in replicas of 4 wells and the experiments were repeated 4 times. Cell viability was determined by thiazolyl blue tetrazolium bromide assay, and the 50% inhibitory concentration (IC50) was calculated (Figure 1). In terms of Vistusertib, the IC50 was (251.6 ± 34.2) nM for NCI-H2452 cells and (98.5 ± 10.3) nM for HEI193 cells, respectively. As for Trametinib, the IC50 was (10.1 ± 2.3) nM for NCI-H2452 cells and (29.6 ± 5.6) nM for HEI193 cells, respectively.

Cell Proliferation Test

HEI193 cells and NCI-H2452 cells were seeded in 96-well cell culture plates with 1×10^4 cells per well in 100 µL medium with 10% serum overnight. All cells were divided into four groups, the control group (DMSO added), the T group (Trametinib of IC50 concentration added), the V group (Vistusertib of IC50 concentration added) and the V+T group (Trametinib and Vistusertib of IC50 concentration added). Cell viability was measured by CCK-8 kit (Beyotime Biological Engineering Co., Ltd., Shanghai, China) according to the manufacturer's instruction. The absorbance at 490 nm with a 690-nm reference was measured with a Molecular Device Spectra Max M4 Microplate Reader (Tecan, Morrisville, NC, USA). Relative cell viability was calculated with the NC-transfected cells as controls. Experiments were repeated at least twice[15]. Before measuring the absorbance of different groups, the cells were captured via bright field microscope, and pictures were taken using a 2.5x objective on a Carl Zeiss Axiocam MRc, which were shown in Figure 2A (HEI193) and 2B (NCI-H2452). Compared to the control group (DMSO added), both T group and V group showed relatively less cell number. However, the V+T group had even less cell number than both T group and V group. This result was also confirmed

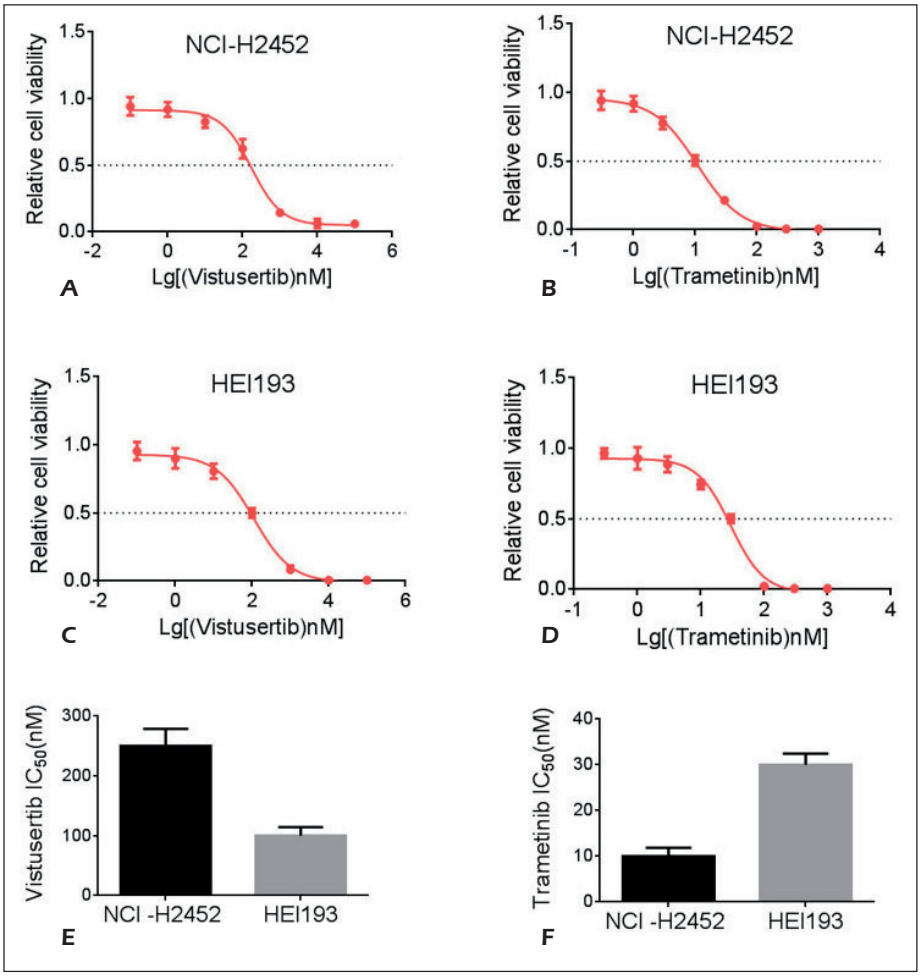

Figure 2. IC50 detection of Vistusertib and Trametinib in HEI193 cells and NCI-H2452 cells. **A**, Cell viability changes according to different concentration of Vistusertib in NCI-H2452 cells; **B**, Cell viability changes according to different concentration of Trametinib in NCI-H2452 cells; **C**, Cell viability changes according to different concentration of Vistusertib in HEI193 cells; **D**, Cell viability changes according to different concentration of Trametinib in HEI193 cells. **E**, IC50 of Vistusertib in HEI193 cells and NCI-H2452 cells; **F**, IC50 of Trametinib in HEI193 cells and NCI-H2452 cells.

by the CCK-8 test, the cell proliferation curve was depicted according to absorbance in different time point after the seeding. Two-way ANOVA was conducted to compare the relative OD value of four groups, which demonstrated a significant difference among them in proliferation curves (all $p<0.001$). Post-hoc test was also conducted to compare each group with the control group. In the experiment of HEI193 cell (Figure 2C), the relative OD value of both T group and V group was significantly lower than that of the control group (both $p<0.01$), while the relative OD value of V+T group was even more significantly lower than that of the control group ($p<0.005$). In the experiment of NCI-H2452 cells (Figure 2D), the relative OD values of both T group, V group and V+T group were significantly lower than that of the control group (all $p<0.01$).

Tumorigenicity Inhibition

Twenty-four healthy female BALB/c Nude mice (4 weeks old) were divided into four groups, the control group, the T group, the V group and the V+T group (6 mice each group). All groups of mice were given injection of HEI193 cells (4×10^6 cells per mouse) subcutaneously on the right flank of each mouse. After 5 days, different groups were given different treatments via caudal veins every three days: the control group was given PBS, the T group given Trametinib (0.2 mg/kg), the V group given Vistusertib (0.5 mg/kg) and the V+T group given (0.2 mg/kg Trametinib and 0.5 mg/kg Vistusertib). Tumor volume (V) was calculated every five days via measuring the length (L) and width (W) with vernier caliper ($V = L\times W^2\times0.5$). After 25 days of the injection, the mice were sacrificed, and the tumors were removed and measured of weight.

The *in vivo* tumorigenicity results were shown in Figure 3. The tumor size was significantly reduced by the application of Trametinib, or Vistusertib, or Trametinib and Vistusertib together (Figure 3A). The tumor growth curve also demonstrated that no matter Trametinib, or Vistusertib, or combined together, all could significantly inhibit the tumor growth formed by HEI193 cells (all $p<0.01$) (Figure 3B). However, the combination of Trametinib and Vistusertib could mostly reduce the tumor growth compared with Trametinib or Vistusertib alone ($p<0.001$). After 25 days, tumors in nude mice were removed and weighed, further showing that tumor weights of V group, T group, and V+T group were significantly lower than that of the control group, while V+T group had the lowest tumor weight among all four groups (Figure 3C and 3D).

Apoptosis Induction

Cell Culture and Flow Cytometry

HEI193 cell lines and NCI-H2452 cell lines were cultured as described above. HEI193 cells and NCI-H2452 cells were seeded at 1.5.105 cells/well in 24-well plates (TPP). All cells were divided into four groups, the control group (DMSO added), the T group (Trametinib of IC50 concentration added), the V group (Vistusertib of IC50 a concentration added) and the V+T group (Trametinib and Vistusertib of IC50 concentration added). Annexin V and propidium iodide (PI) staining were performed using Alexa Fluor® 488 Annexin V/Dead Cell Apoptosis Kit (Thermo Fisher Scientific, Waltham, MA, USA) according to the manufacturer's instructions. The samples were analyzed by flow cytometry on a FACSCanto II cytometer using FACSDiva software v6.1.3 (BD Biosciences, Franklin Lakes, NJ, USA). Comparison of apoptosis ratio was conducted with Student-*t* test. $p<0.05$ was considered as statistically significant.

The apoptosis results were shown in Figure 4 and Figure 5. The apoptosis ratio of both T group and V group was significantly higher than the control group for HEI193 cells ($p<0.01$), while that of the V+T group was even more significantly higher than the control group ($p<0.005$) (Figure 4A and 4C). In terms of NCI-H2452 cells, all experimental groups including T group, V group and V+T group showed higher apoptosis ratios than the control group (all $p<0.01$) (Figure 4B and 4D). Notably, the apoptosis ratios were higher in V+T group than single T group and V group.

PI3K/mTOR/MEK Pathway Inhibition

Western blot for related proteins including AKT, ERK, MEK, PI3K, mTOR and phosphorylated ones, as well as Merlin and GAPDH, was conducted according to previously reported methods, when total proteins were harvested from cultured NCI-H2452 cells and HEI193 cells in 7 days. All antibodies were purchased from Abcam (Cambridge, MA, USA). ImageJ was used to quantify the optical density of different bands, when all proteins relative fold changes were calculated by dividing with GAPDH. One way ANOVA was used to compare the optical density of different groups. For NCI-H2452 cells, the expression level of AKT, ERK, MEK, PI3K, mTOR was similar among the control group (PBS added), the T

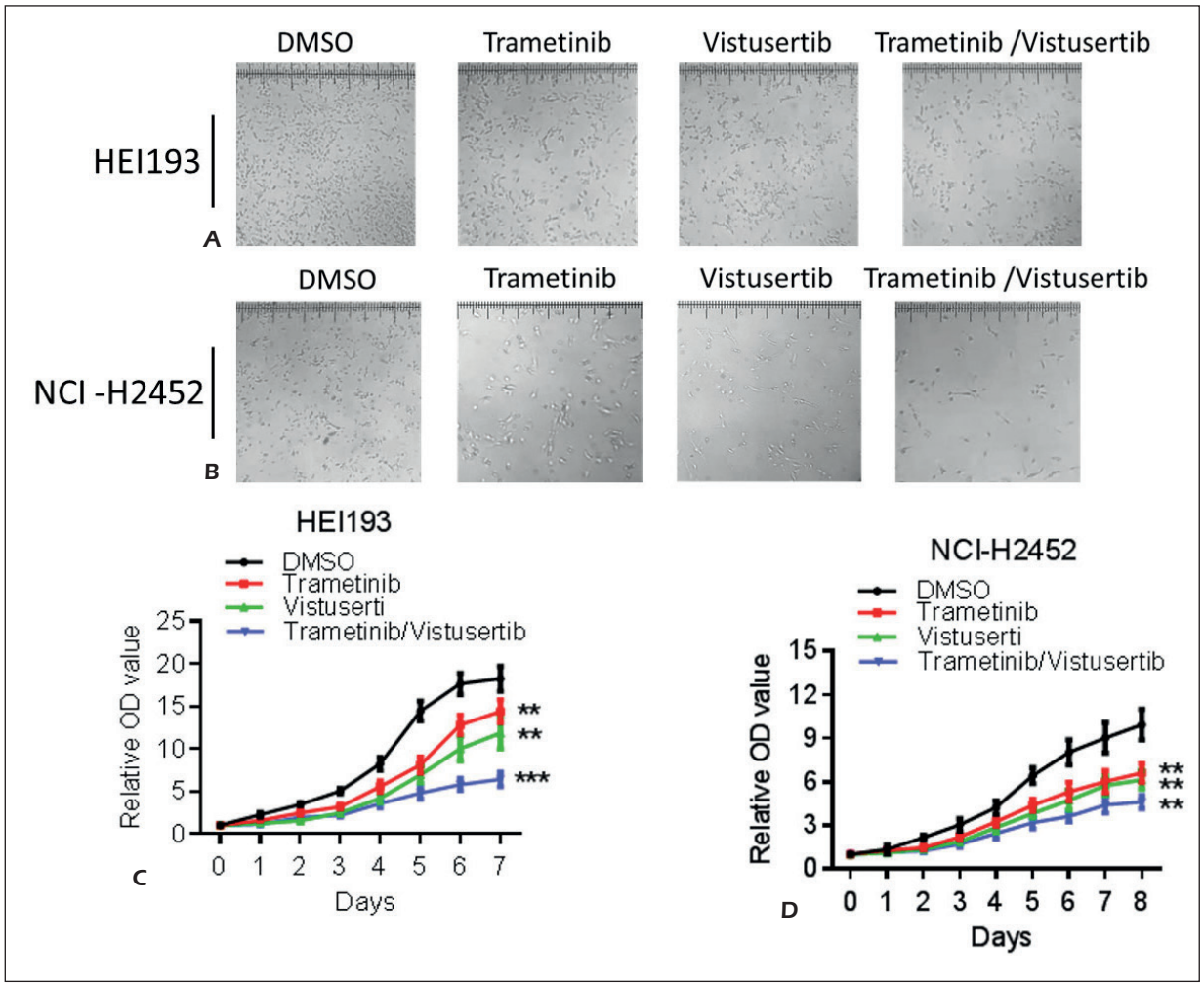

Figure 3. Cell proliferation examinations of different treatments. **A**, Bright field microscope pictures of HEI193 cells under different treatments. **F**, Bright field microscope pictures of NCI-H2452 cells under different treatments. **C**, Cell proliferation curve of HEI193 cells under different treatments. **D**, Cell proliferation curve of NCI-H2452 cells under different treatments. *p<0.05, **p<0.01, ***p<0.005.

group (Trametinib of IC50 concentration added), the V group (Vistusertib of IC50 a concentration added) and the V+T group (Trametinib and Vistusertib of IC50 concentration added). However, the expression level of phosphorylated proteins was significantly different among the four groups. The expression levels of p-mTOR of the T group, the V group, and the V+T group were all lower than the control group (p<0.001) (Figure 6). For p-ERK and p-MEK, there was no difference between the T group and the control group (p>0.05). However, p-ERK and p-MEK of the V group, and the V+T group were significantly lower than the control group (p<0.001). Notably, the merlin was significantly increased in three groups than the control group (p<0.001). Similar results were also acquired in for the HEI193 cells.

Discussion

In this study, using the NF-2 mutation cell model of HEI193 cells and NCI-H2452 cells, we investigated the effect of two PI3K/mTOR inhibitors on the proliferation and apoptosis of cell models, and found the following results: 1) for both HEI193 cells and NCI-H2452 cells, Trametinib could significantly inhibit the cell proliferation and induce apoptosis; 2) for both HEI193 cells and NCI-H2452 cells, Vistusertib could also inhibit the cell proliferation and induce apoptosis; 3) when Trametinib and Vistusertib are combined together, a more significant effect could be achieved on cell proliferation inhibition and apoptosis induction. Numerous studies have been launched to investigate the potential mechanism underlying the suppressing

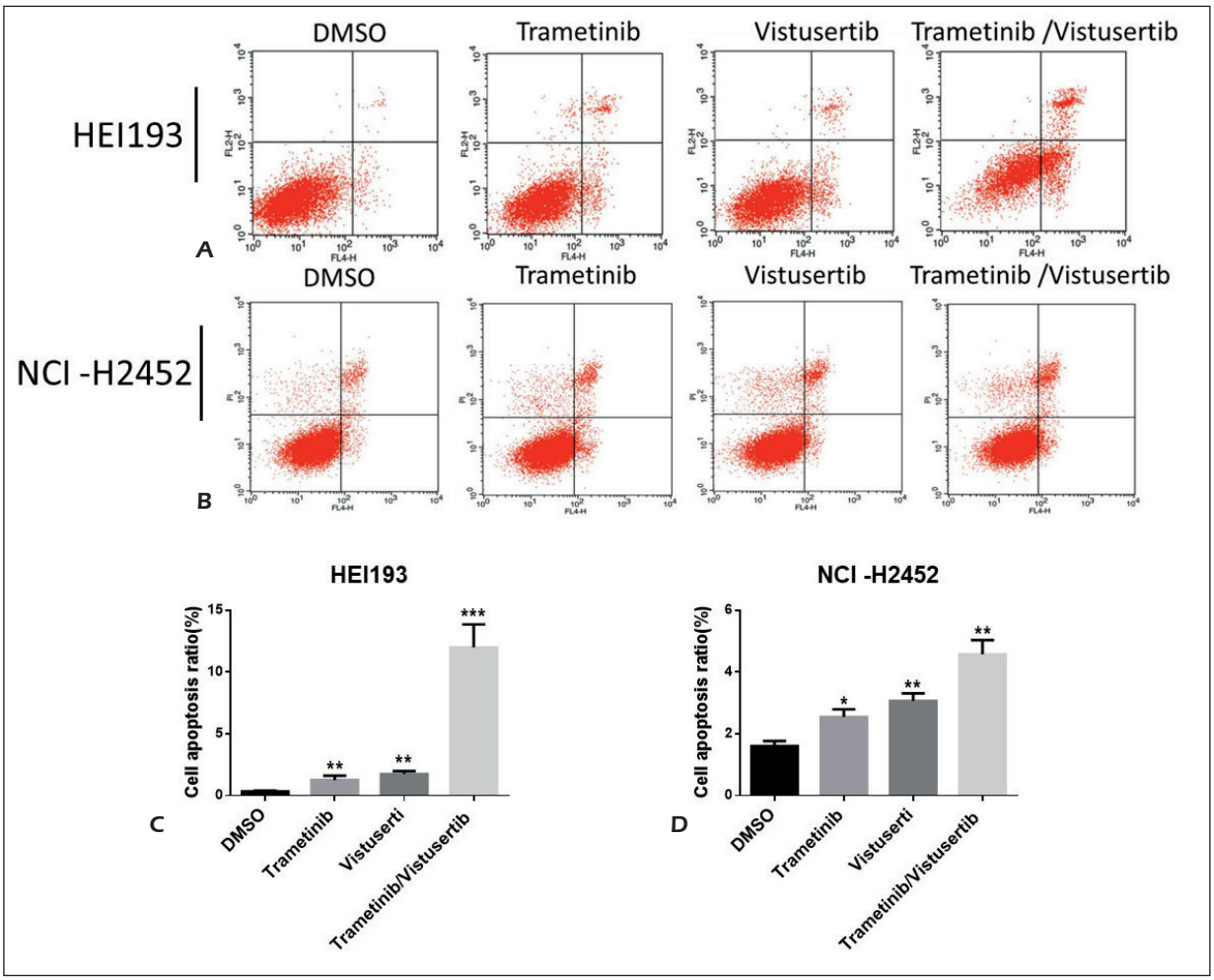

Figure 4. Tumor formation results in nude mice. **A**, Tumor formation of different groups 25 days after injection of HEI193 cells; **B**, Tumor volume changes of different groups after the injection of HEI193 cells; **C**, Comparison of dissected tumors of different groups 25 days after injection of HEI193 cells.; **D**, Tumor weight of different groups 25 days after injection of HEI193 cells. 6 mice each group, $^{**}p<0.01$, $^{***}p<0.005$, compared with controls.

role of merlin in tumor development. Stokowski et al[19] found that 80% of the merlin mutants studied significantly altered cell adhesion, causing cells to detach from the substratum. This finding implies a function for merlin in regulating cell-matrix attachment, and changes in cell adhesion caused by mutant protein expression may be an initial step in the pathogenesis of NF2[19]. Another study examined the role of NF2/Merlin in sporadic colorectal cancer through LOH analysis at the NF2 locus and mRNA expression analysis via quantitative RT-PCR of total NF2, NF2 isoform, and results showed that NF2/Merlin may serve as a potential target in the management of colorectal cancer. All the above data demonstrated a potential target of NF-2 mutation related tumors. We used string database to find the most related targeted sites, which demonstrated that PI3K/mTOR pathway was tightly associated with NF-2 mutation. Yesilöz et al[20] also found that patients with skull base meningiomas with NF-2 mutation might benefit from additional treatment targeting the mTOR pathway.

PI3K/mTOR or PI3K/mTOR/MEK pathway is a fully studied classic molecular signaling pathway, which plays an important role in human physiology, while activated in several tumor types including breast cancer[21], prostate cancer[22], gastric cancer[23], thyroid cancer[24], and colon cancer[25]. Therefore, drugs targeting PI3K/mTOR/MEK pathway have been developed to treat cancers[26-28]. Vistusertib (AZD2014) is a kind of mTOR kinase inhibitor, which was demonstrated to be effective in inducing apoptosis for cisplatin- resistant model (A2780Cis) of ovarian cancer. Following

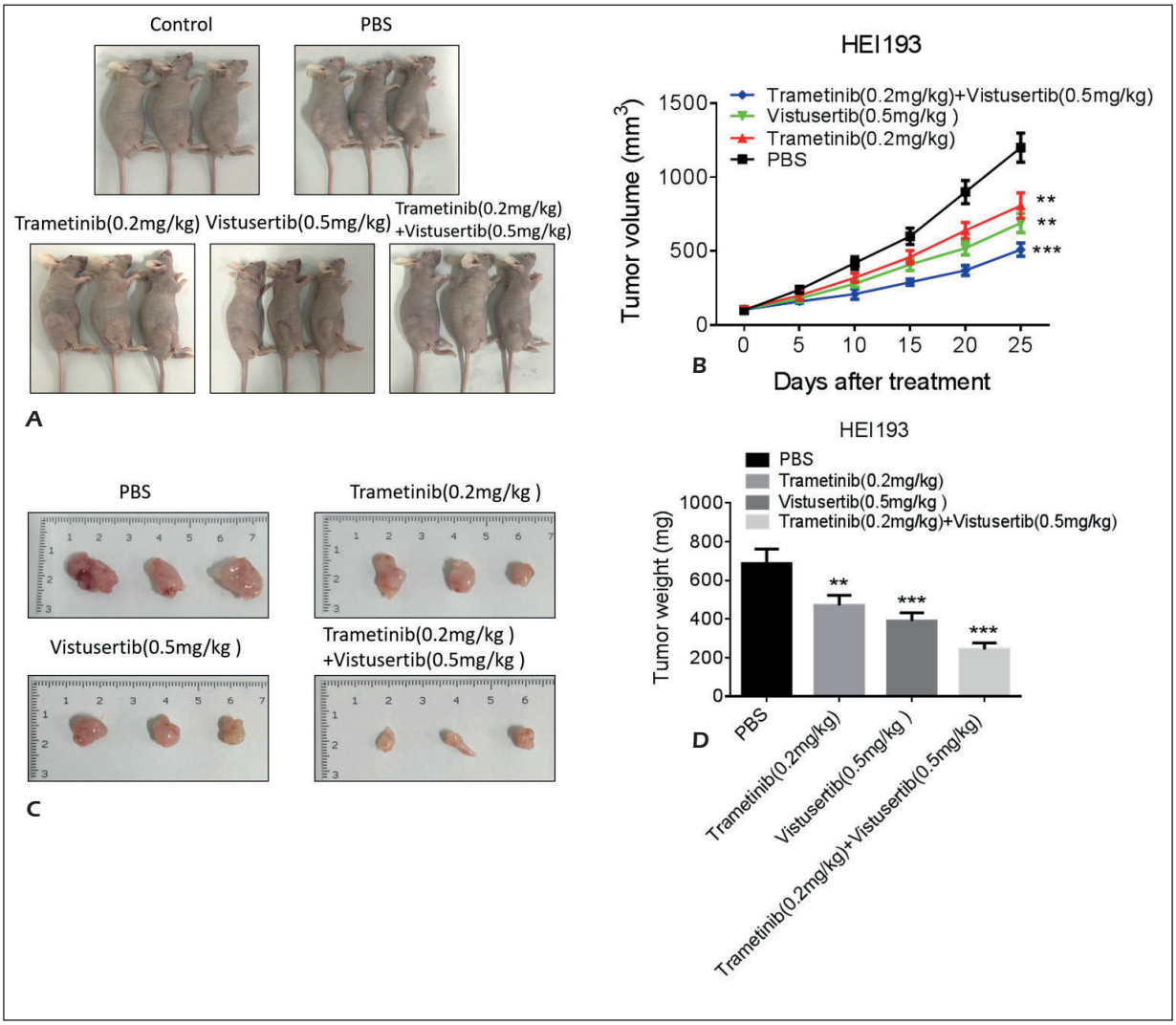

Figure 5. Apoptosis examined by flow cytometry. **A**, Apoptosis of HEI193 cells was induced by different treatments. **B**, Apoptosis of NCI-H2452 cells was induced by different treatments. **C**, Comparison of cell apoptosis ratio among different groups of HEI193 cells. **D**, Comparison of cell apoptosis ratio among different groups of NCI-H2452 cells. *$p<0.05$, **$p<0.01$, ***$p<0.005$.

clinical trials also proved that the combination of Vistusertib on paclitaxel could benefit the patient of ovarian cancer[29]. Our study focused on cell proliferation and apoptosis, which were the most useful models in researching cancer. The results showed that Vistusertib along could significantly inhibit the cell growth of two kinds of NF-2 mutation cell lines, including HEI193 cells and NCI-H2452 cells, which was considered as the most typical NF-2 mutation cell lines[30]. Cell flow cytometry results demonstrated that Vistusertib could lead to apoptosis. Apoptosis is an important physiological process of cell death, while mitigation of apoptosis can be one key pathological cause of tumorigenesis[31]. Wang et al[32] demonstrated that pharmacological inhibition of RAC1 could significantly inhibit the proliferation of both RT4 cells and human NF2-associated primary schwannoma cells by inducing apoptosis.

Similar results were also achieved for Trametinib. Unlike Vistusertib, Trametinib is a MEK inhibitor which was proven to be effective in the treatment of advanced BRAF (V600) mutant melanoma[33]. Combination treatment of other drugs such as BRAF inhibitors with Trametinib was also developed to achieve better prognosis for metastatic melanoma[13]. Our results also showed that the treatment of Trametinib with IC50 con-

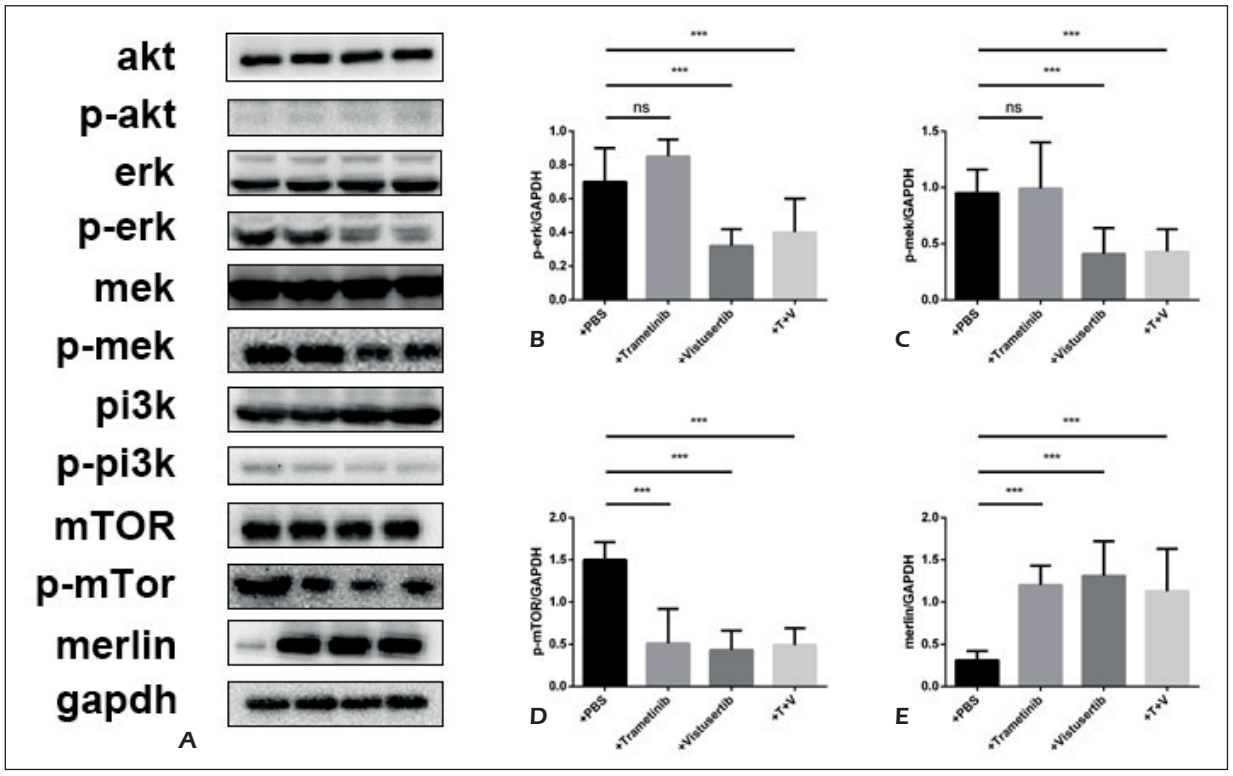

Figure 6. Western blot results of the control group, the T group, the V group, and the V+T group for NCI-H2452 cells. **A**, Representative WB bands of four groups; **B**, Relative optical density of p-ERK of four groups; **C**, Relative optical density of p-MEK of four groups; **D**, Relative optical density of p-mTOR of four groups; **E**, Relative optical density of Merlin of four groups. ns, not significant. ***$p<0.001$.

centration could significantly inhibit cell proliferation and induce apoptosis, which was in agree with other reports. Notably, the combination of two drugs could significantly increase the level of proliferation inhibition and apoptosis induction. Although both Vistusertib and Trametinib act on PI3K/mTOR pathway, they focused on different functional sites, which have a synergic effect on cell growth inhibition and apoptosis. However, the underlying mechanism of their synergic effect requires further investigation. Except for the *in vitro* cell studies, a tumorigenesis experiment *in vivo* was also conducted in this work to further validate our hypothesis, of which the results were in agree with *in vitro* experiments. The Western blots results revealed the PI3K/mTOR pathway inhibition by the combination of Vistusertib and Trametinib, as well as the increase of merlin expression. Those results validated our suggestion that NF-2 mutation was associated with PI3K/mTOR pathway, and the adoption of PI3K/mTOR pathway inhibitor could increase Merlin expression and enhance apoptosis of tumor cells, implicating that those drugs and pathway might be potential targets for NF-2 mutation related cancer.

Although several findings have been acquired, there are some limitations: 1. Although Trametinib and Vistusertib were proven effective on NF-2 mutation tumor, more clinical evidence is required to confirm those results. 2. The reason why Vistusertib and Trametinib could inhibit cell proliferation and enhance apoptosis needs deeper research. 3. The synergic effect of two drugs also needs more fundamental studies to confirm.

Conclusions

We demonstrated that whether Vistusertib or Trametinib - PI3K/mTOR pathway inhibitor – could significantly decrease the proliferation activity of NF-2 mutation tumor cell line, and they have a stronger synergic effect when combined.

Acknowledgement

Ning Li and Xinyi Lu equally contributed to this paper. This study was supported by grants from the National Natural Science Foundation of China (No. 81472551).

Conflict of Interests

The authors declare no conflict of interest

References

1) Sondka Z, Bamford S, Cole CG, Ward SA, Dunham I, Forbes SA. The COSMIC Cancer Gene Census: describing genetic dysfunction across all human cancers. Nat Rev Cancer 2018; 18: 696-705.
2) Okada T, You L, Giancotti FG. Shedding light on Merlin's wizardry. Trends Cell Biol 2007; 17: 222-229.
3) Wolff RK, Frazer KA, Jackler RK, Lanser MJ, Pitts LH, Cox DR. Analysis of chromosome 22 deletions in neurofibromatosis type 2-related tumors. Am J Hum Genet 1992; 51: 478-485.
4) Mehra R, Vats P, Cieslik M, Cao X, Su F, Shukla S, Udager AM, Wang R, Pan J, Kasaian K, Lonigro R, Siddiqui J, Premkumar K, Palapattu G, Weizer A, Hafez KS, Wolf JS Jr, Sangoi AR, Trpkov K, Osunkoya AO, Zhou M, Giannico G, McKenney JK, Dhanasekaran SM, Chinnaiyan AM. Biallelic alteration and dysregulation of the hippo pathway in mucinous tubular and spindle cell carcinoma of the kidney. Cancer Discov 2016; 6: 1258-1266.
5) Pal SK, Choueiri TK, Wang K, Khaira D, Karam JA, Van Allen E, Palma NA, Stein MN, Johnson A, Squillace R, Elvin JA, Chmielecki J, Yelensky R, Yakirevich E, Lipson D, Lin DI, Miller VA, Stephens PJ, Ali SM, Ross JS. Characterization of clinical cases of collecting duct carcinoma of the kidney assessed by comprehensive genomic profiling. Eur Urol 2016; 70: 516-521.
6) Tranchant R, Quetel L, Tallet A, Meiller C, Renier A, de Koning L, de Reynies A, Le Pimpec-Barthes F, Zucman-Rossi J, Jaurand MC, Jean D. Co-occurring mutations of tumor suppressor genes, LATS2 and NF2, in malignant pleural mesothelioma. Clin Cancer Res 2017; 23: 3191-3202.
7) Paganini I, Capone GL, Vitte J, Sestini R, Putignano AL, Giovannini M, Papi L. Double somatic SMARCB1 and NF2 mutations in sporadic spinal schwannoma. J Neurooncol 2018; 137: 33-38.
8) Ali SM, Miller VA, Ross JS, Pal SK. Exceptional response on addition of everolimus to taxane in urothelial carcinoma bearing an NF2 mutation. Eur Urol 2015; 67: 1195-1196.
9) Pineau P, Marchio A, Nagamori S, Seki S, Tiollais P, Dejean A. Homozygous deletion scanning in hepatobiliary tumor cell lines reveals alternative pathways for liver carcinogenesis. Hepatology 2003; 37: 852-861.
10) Kraus JA, de Millas W, Sörensen N, Herbold C, Schichor C, Tonn JC, Wiestler OD, von Deimling A, Pietsch T. Indications for a tumor suppressor gene at 22q11 involved in the pathogenesis of ependymal tumors and distinct from hSNF5/INI1. Acta Neuropathol 2001; 102: 69-74.
11) Čačev T, Aralica G, Lončar B, Kapitanović S. Loss of NF2/Merlin expression in advanced sporadic colorectal cancer. Cell Oncol (Dordr) 2014; 37: 69-77.
12) Cooper J, Xu Q, Zhou L, Pavlovic M, Ojeda V, Moulick K, de Stanchina E, Poirier JT, Zauderer M, Rudin CM, Karajannis MA, Hanemann CO, Giancotti FG. Combined inhibition of NEDD8-activating enzyme and mTOR suppresses NF2 loss-driven tumorigenesis. Mol Cancer Ther 2017; 16: 1693-1704.
13) Lugowska I, Koseła-Paterczyk H, Kozak K, Rutkowski P. Trametinib: a MEK inhibitor for management of metastatic melanoma. Onco Targets Ther 2015; 8: 2251-2259.
14) Basu B, Krebs MG, Sundar R, Wilson RH, Spicer J, Jones R, Brada M, Talbot DC, Steele N, Ingles Garces AH, Brugger W, Harrington EA, Evans J, Hall E, Tovey H, de Oliveira FM, Carreira S, Swales K, Ruddle R, Raynaud FI, Purchase B, Dawes JC, Parmar M, Turner AJ, Tunariu N, Banerjee S, de Bono JS, Banerji U. Vistusertib (dual m-TORC1/2 inhibitor) in combination with paclitaxel in patients with high-grade serous ovarian and squamous non-small-cell lung cancer. Ann Oncol 2018; 29: 1918-1925.
15) Ju L, Wu W, Yin X, Xiao Y, Jia Z, Lou J, Yu M, Ying S, Chen T, Jiang Z, Li W, Chen J, Zhang X, Zhu L. miR-30d is related to asbestos exposure and inhibits migration and invasion in NCI-H2452 cells. FEBS Open Bio 2017; 7: 1469-1479.
16) Wong HK, Lahdenranta J, Kamoun WS, Chan AW, McClatchey AI, Plotkin SR, Jain RK, di Tomaso E. Anti-vascular endothelial growth factor therapies as a novel therapeutic approach to treating neurofibromatosis-related tumors. Cancer Res 2010; 70: 3483-3493.
17) Hermanek P. The superiority of the new International Union Against Cancer and American Joint Committee on Cancer TNM staging of gastric carcinoma. Cancer 2000; 88: 1763-1765.
18) Bader GD, Hogue CW. An automated method for finding molecular complexes in large protein interaction networks. BMC Bioinformatics 2003; 4: 2.
19) Stokowski RP, Cox DR. Functional analysis of the neurofibromatosis type 2 protein by means of disease-causing point mutations. Am J Hum Genet 2000; 66: 873-891.
20) Yesilöz Ü, Kirches E, Hartmann C, Scholz J, Kropf S, Sahm F, Nakamura M, Mawrin C. Frequent AKT1E17K mutations in skull base meningiomas are associated with mTOR and ERK1/2 activation and reduced time to tumor recurrence. Neuro Oncol 2017; 19: 1088-1096.
21) Kenna MM, McGarrigle S, Pidgeon GP. The next generation of PI3K-Akt-mTOR pathway inhibitors in breast cancer cohorts. Biochim Biophys Acta Rev Cancer 2018; 1870: 185-197.
22) Park S, Kim YS, Kim DY, So I, Jeon JH. PI3K pathway in prostate cancer: all resistant roads lead to PI3K. Biochim Biophys Acta Rev Cancer 2018; 1870: 198-206.
23) Ito C, Nishizuka SS, Ishida K, Uesugi N, Sugai T, Tamura G, Koeda K, Sasaki A. Analysis of PIK3CA mutations and PI3K pathway proteins in advanced gastric cancer. J Surg Res 2017; 212: 195-204.

24) Liu D, Shen X, Zhu G, Xing M. REC8 is a novel tumor suppressor gene epigenetically robustly targeted by the PI3K pathway in thyroid cancer. Oncotarget 2015; 6: 39211-39224.
25) Ma J, Su H, Yu B, Guo T, Gong Z, Qi J, Zhao X, Du J. CXCL12 gene silencing down-regulates metastatic potential via blockage of MAPK/PI3K/AP-1 signaling pathway in colon cancer. Clin Transl Oncol 2018; 20: 1035-1045.
26) Stratikopoulos EE, Parsons RE. Molecular pathways: targeting the PI3K pathway in cancer-BET inhibitors to the rescue. Clin Cancer Res 2016; 22: 2605-2610.
27) Li H, Zeng J, Shen K. PI3K/AKT/mTOR signaling pathway as a therapeutic target for ovarian cancer. Arch Gynecol Obstet 2014; 290: 1067-1078.
28) Bahrami A, Khazaei M, Hasanzadeh M, ShahidSales S, Joudi Mashhad M, Farazestanian M, Sadeghnia HR, Rezayi M, Maftouh M, Hassanian SM, Avan A. Therapeutic potential of targeting PI3K/AKT pathway in treatment of colorectal cancer: rational and progress. J Cell Biochem 2018; 119: 2460-2469.
29) Wong Te Fong AC, Thavasu P, Gagrica S, Swales KE, Leach MO, Cosulich SC, Chung YL, Banerji U. Evaluation of the combination of the dual m-TORC1/2 inhibitor vistusertib (AZD2014) and paclitaxel in ovarian cancer models. Oncotarget 2017; 8: 113874-113884.
30) Guo J, Grovola MR, Xie H, Coggins GE, Duggan P, Hasan R, Huang J, Lin DW, Song C, Witek GM, Berritt S, Schultz DC, Field J. Comprehensive pharmacological profiling of neurofibromatosis cell lines. Am J Cancer Res 2017; 7: 923-934.
31) Kim JY, Song JJ, Kwon BM, Lee JD. Tanshinone IIA exerts antitumor activity against vestibular schwannoma cells by inhibiting the expression of hypoxia-inducible factor-1alpha. Mol Med Rep 2015; 12: 4604-4609.
32) Wang Y, Wang B, Li P, Zhang Q, Liu P. Reduced RAC1 activity inhibits cell proliferation and induces apoptosis in neurofibromatosis type 2(NF2)-associated schwannoma. Neurol Res 2017; 39: 1086-1093.
33) Thota R, Johnson DB, Sosman JA. Trametinib in the treatment of melanoma. Expert Opin Biol Ther 2015; 15: 735-747.